AD-A066 107 TECHNICAL LIBRARY

AD

TECHNICAL REPORT ARBRL-TR-02130

A PREDICTIVE SCHEME FOR THE BLAST ENVIRONMENT OF ARMY WEAPONS PART II. APPLICATIONS

Dennis Keefer
Bruce Henriksen

January 1979

US ARMY ARMAMENT RESEARCH AND DEVELOPMENT COMMAND
BALLISTIC RESEARCH LABORATORY
ABERDEEN PROVING GROUND, MARYLAND

Approved for public release; distribution unlimited.

Destroy this report when it is no longer needed.
Do not return it to the originator.

Secondary distribution of this report by originating or sponsoring activity is prohibited.

Additional copies of this report may be obtained from the National Technical Information Service, U.S. Department of Commerce, Springfield, Virginia 22161.

The findings in this report are not to be construed as an official Department of the Army position, unless so designated by other authorized documents.

The use of trade names or manufacturers' names in this report does not constitute indorsement of any commercial product.

REPORT DOCUMENTATION PAGE

READ INSTRUCTIONS BEFORE COMPLETING FORM

1. REPORT NUMBER: TECHNICAL REPORT ARBRL-TR-02130
2. GOVT ACCESSION NO.
3. RECIPIENT'S CATALOG NUMBER

4. TITLE (and Subtitle): A Predictive Scheme for the Blast Environment of Army Weapons, Part II. Applications
5. TYPE OF REPORT & PERIOD COVERED
6. PERFORMING ORG. REPORT NUMBER

7. AUTHOR(s): Dennis Keefer
Bruce Henriksen

8. CONTRACT OR GRANT NUMBER(s)

9. PERFORMING ORGANIZATION NAME AND ADDRESS: US Army Ballistic Research Laboratory (DRDAR-BLB)
Aberdeen Proving Ground, MD 21005

10. PROGRAM ELEMENT, PROJECT, TASK AREA & WORK UNIT NUMBERS: 1L162618AH80

11. CONTROLLING OFFICE NAME AND ADDRESS: US Army Armament Research & Development Command
US Army Ballistic Research Laboratory
(ATTN: DRDAR-BL)
Aberdeen Proving Ground, MD 21005

12. REPORT DATE: JANUARY 1979
13. NUMBER OF PAGES: 54

14. MONITORING AGENCY NAME & ADDRESS (if different from Controlling Office)

15. SECURITY CLASS. (of this report): Unclassified
15a. DECLASSIFICATION/DOWNGRADING SCHEDULE

16. DISTRIBUTION STATEMENT (of this Report)

Approved for public release; distribution unlimited.

17. DISTRIBUTION STATEMENT (of the abstract entered in Block 20, if different from Report)

18. SUPPLEMENTARY NOTES

19. KEY WORDS (Continue on reverse side if necessary and identify by block number)

Muzzle blast
Unified Theory of Explosions
Overpressure
Pulse length

20. ABSTRACT (Continue on reverse side if necessary and identify by block number)

This report presents an application of the theories developed in Part I to guns ranging in diameter from .30 caliber to 8 inches. Agreement between theory and experiment is good over the entire diameter range for the blast field overpressure. The theory was also applied to a 105mm howitzer of different loadings with equally good results.

A different approach for determining the pulse length is presented. As with the data in Part I, the scatter is sufficiently large that no firm conclusions can be drawn concerning the validity of the approach.

TABLE OF CONTENTS

		Page
I.	INTRODUCTION	5
II.	THEORY	6
	II.1 Interior Analysis	6
	II.2 Blast Wave Analysis	12
	II.2a The Unified Theory of Explosions	13
	II.2b Asymmetric Blast Effects	16
	II.3 Pulse Length Calculations	17
III.	RESULTS	24
	III.1 Guns Considered	24
	III.2 Comparison of Theory and Experiment	26
	REFERENCES	36
	APPENDIX	37
	DISTRIBUTION LIST	45

I. Introduction

Knowledge of the blast field produced by Army guns is becoming increasingly important as attempts are made to increase range and muzzle velocity. While these attributes are important to the lethality of the weapon system, the accompanying side effect -- stronger muzzle blast field -- can prove detrimental to the launch platform as well as the firing personnel.

Heretofore information on the blast field strength was obtained from either actual firings (expensive), scaling parameters (always suspect for new systems because they are often empirical in nature) or from hydrocodes (expensive and oftentimes questioned). In Part I a model was developed to predict the blast field which was simple and economical to use and which provided insight into the relevant physical processes [1].

This part presents an overview of the analysis with application to guns ranging in barrel diameter from .30 caiber to 8 inch.

---

[1] B. Henriksen, B. Cummings,"A Predictive Scheme for the Blast Environment of Army Weapons, Part I. Devlopment and Validation of the Theory," BRL Technical Report ARBRL-TR-02044, Feb. 1978. (AD #A053487)

II. Theory

The approach in predicting the blast overpressure consists of two parts: (1) analysis of the interior losses leading to a prediction of an equivalent yield for a spherical explosion at the muzzle and (2) analysis of the blast wave from the explosion with suitable modifications to account for the geometric asymmetries introduced by the high exit velocity of the gases. The following is designed to give an overview of the analysis -- the details are contained in Reference 1.

The analysis is an accounting of the energies in the firing process. Fundamental to the theory is the partitioning of energy into either prompt energy or waste heat. Prompt energy is that energy which is "promptly" available for supporting the shock wave. It consists of the static overpressure and the dynamic pressure. Waste heat includes all other energies. Examples of this type are: energies which for some reason are delayed; energies which appear as ambient temperature rise; energies which perform irreversible work such as crushing a material, etc. This division of energies is important because it allows focusing the analysis only on the prompt energy -- once an energy is determined to be waste heat it can be excluded from the analysis.

The following two sections address the interior losses and the blast wave predictions for the equivalent explosion at the muzzle.

II.1 Interior Analysis

The losses from the initial total propellant energy are grouped as follows:

a) energy imparted to the projectile,
b) energy lost to the barrel in the form of recoil, barrel heating, barrel expansion, etc.,
c) energy converted to waste heat by formation of the boundary layer, and
d) energy trapped in the grooves (rifling).

Energy loss a) is self-evident. The projectile energy does not support the main blast wave. A certain amount of the energy does appear as a shock wave off the projectile; however, this is not the strong, damage-producing wave.

Energy loss b): This loss is estimated from experience with conical shock tubes. Measurements show that only about 16% of the initial explosive energy is imparted to the shock wave. This can be visualized with the help of Figure 1. If we view the propellant as a cube and equipartition the direction of energy flow we see that 1/6 is

directed towards the muzzle, 2/3 is directed to the walls and 1/6 is directed towards the rear (recoil). We are not suggesting that the 5/6 portion of the energy does not exit the tube, only that it is delayed and hence is not promptly available.

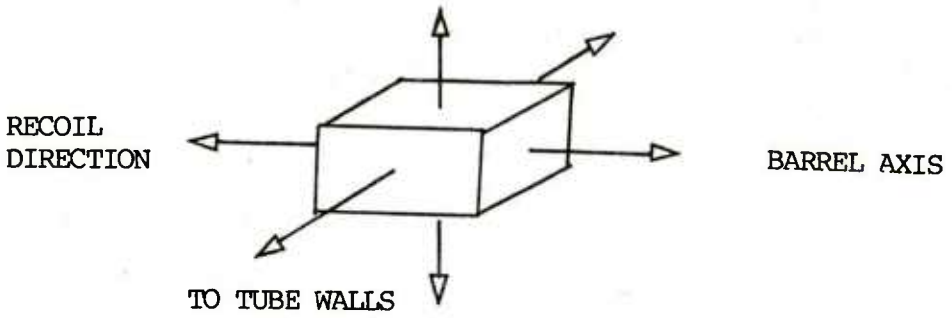

Figure 1

Energy loss c): We propose that as the projectile travels down the barrel a boundary layer is formed as depicted in Figure 2.

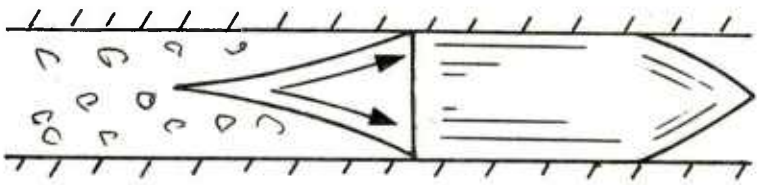

Figure 2

The boundary layer closure divides the flow into two distinct regions. In the boundary layer the flow is turbulent with the energy partitioned between the three translational degrees of freedom. In the conical region between the closure point and the projectile the motion of the fluid particles is ordered and traveling in the direction of the projectile. We propose that the strength of the blast wave is determined by the pressure in the fluid at the projectile base. In the turbulent boundary layer a fluid particle has a probability of traveling in any of the three directions; hence we treat this energy as delayed.

We can estimate the pressure at the projectile base by treating the ordered flow region as consisting of an expansion from the closure point where the ordered motion is essentially zero (in a reference frame associated with the projectile) to some velocity at the projectile base. To make the analysis tractable we assume there are no expansion or compression waves in this region and apply the approach of Bernoulli to this expansion process.

Since we are interested in motion only along the barrel axis (z axis) the appropriate differential equation is

$$\frac{\partial P}{\partial z} + \rho\, u\, \frac{\partial u}{\partial z} + \rho\, \frac{\partial u}{\partial t} = 0, \qquad \text{(II.1.1)}$$

in which the ordered velocity is represented by u.

In Part I an examination of experimental data showed that the thermal velocity of the fluid particles in random motion is of the same order as the projectile velocity. This suggests that the distance from the closure point to the projectile base is constant with the consequence that the temporal variation of u is negligible.

Equation (II.1.1) becomes an ordinary differential equation and, with the use of the adiabatic expansion relations, can be integrated to yield

$$\frac{2}{\gamma - 1}\, a^2 + u^2 = \text{constant} \qquad \text{(II.1.2)}$$

where γ is the ratio of the specific heats and a is the speed of sound. The constant is evaluated by noting that at the closure point the ordered velocity is essentially zero (stagnated) and hence we associate the pressure at that point with the chamber pressure.

After some algebra we find that the pressure ratio at the projectile base can be determined from

$$P_{r_c} = P_{r_p} \left[1 + \frac{(P_{r_c} - 1)^2}{\gamma\, P_{r_p} \left(P_{r_p} + \frac{\gamma+1}{\gamma-1} \right)} \right]^{\frac{\gamma}{\gamma - 1}} \qquad \text{(II.1.3)}$$

where P_r denotes the pressure ratio relative to ambient and the subscripts c and p refer to the chamber and projectile respectively. For large chamber pressure ratios (>>1) the above relation becomes, approximately,

$$P_{r_c} = 18.9\, P_{r_p}$$

This states that the effect of the choke formation is a reduction in the prompt energy by a factor of approximately 19.

Knowledge of the point at which boundary layer closure occurs is of importance in determining subseqent losses (item d). Experimental results using shock tubes show that the distance down the barrel at which closure occurs can be estimated from the empirical relation [2]

$$\frac{L}{D} = \frac{15}{H^{0.1}}$$

where H is the roughness factor and equal to the ratio of the roughness height (rifling) to the unimpeded diameter of the tube.

The last energy loss mechanism, d, is determined after boundary layer closure has occurred and continues along the remainder of the barrel. The specific process is visualized using Figure 3 in which the rifling is depicted as vertical structures approximating baffles.

Figure 3

The loss mechanism is simply an impedance of the energy flow due to entrapment within the rifling.

---

[2] F.B. Porzel, "Study of Shock Impedance Effects in a Rough Walled Tunnel," IDA Log No. HQ 68-7324, Mar., 1969 (AD 684790).

The analysis determines the change in the total energy. It is assumed proportional to the kinetic energy (per unit volume), ϵ_{KE}, and the volume subtended by the average roughness of the barrel, which itself is a product of the rifling height, h, perimeter s and the distance, dL. That is,

$$dE_T = -\alpha\, \epsilon_{KE}\, s\, h\, dL. \qquad \text{(II.1.4)}$$

Employing the standard relations of compressible flow -- adiabatic, Rankine-Hugoniot, etc. -- Equation (II.1.4) can be integrated to yield

$$\frac{2\beta-1}{\beta} \ln(\Delta P_r) - \frac{\beta-1}{\beta} \ln(\Delta P_r + \beta) - \frac{1}{\Delta P_r} =$$

$$\text{constant} - 2\alpha \frac{h}{D} \frac{L}{D}, \qquad \text{(II.1.5)}$$

where

$$\beta = \frac{2\gamma}{\gamma - 1}$$

and

$$\Delta P_r = P_r - 1,$$

is the overpressure ratio.

The constant can be eliminated by evaluating the expression between two points along the barrel. Specifically, we select the overpressure ratio at the point where the boundary layer closure occurs. This allows us to determine the overpressure ratio at the muzzle. Denoting the left-hand side of Equation (II.1.5) by I, we obtain as the impedance loss between the two points

$$I_1 - I_2 = 2 \alpha \frac{h}{D} \frac{L_2 - L_1}{D} \qquad \text{(II.1.6)}$$

Experimental measurements with shock tubes show that, for barrel lengths of interest, the proportionality constant is equal to unity.[2]

In the present analysis the kinetic energy of the moving gas at the instant the projectile leaves the barrel is included in the hydrodynamic yield. The initial prompt energy of the equivalent explosion is

$$Y_o = \frac{1}{6} \left[(M_p \epsilon - KE) \beta + \frac{1}{2} M_p V_m^2 \right]$$

where Mp is the propellant mass, ϵ is the specific energy of the propellent, KE is the projectile kinetic energy, β is the barrel loss factor as determined from the previous discussion and Vm is the muzzle velocity. An initial value of the explosion radius is required in addition to the initial prompt energy in order to use the QZQ hypothesis (discussed in the next section) to predict the blast overpressures. For the gun muzzle blast, the initial explosion may be considered as the mass of high pressure gas which exits the muzzle immediately after the projectile has left the muzzle. Schlieren photographs taken at these times show a "barrel shock" system whose characteristic size is of the order of two muzzle diameters. Hence, in the present analysis the barrel diameter is taken as the initial radius. Further, the QZQ scaling is relatively insensitive to the initial radius chosen.

II.2 Blast Wave Analysis

The core of the analysis for the blast field is the Unified Theory of Explosions as developed by F.B.Porzel.[3] In essence, the analysis is simply an accounting of the production of waste heat -- the remainder of the initial energy being in the blast wave. The computational procedure can be illustrated using Figure 4. Figure 4 shows the standard Pv diagram for an expansion process.

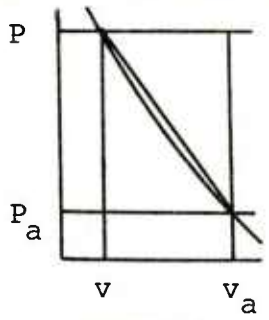

Figure 4

The compressed gas starts at some initial state, Pv. In expanding back to ambient the gas follows the curved line, the so-called Hugoniot or shock adiabat. The straight line connecting the initial and final states represents the thermodynamic path a wave of unchanging shape would follow. The trajectory below the straight line simply states that compression waves steepen while rarefaction waves expand.

From the Rankine-Hugoniot relations, we find that the rectangle bounded by P = constant, v = constant and P = 0, v_a = constant is the total energy:

$$e_T = P\,(v_a - v). \qquad \text{(II.2.1)}$$

The upper triangle in the rectangle is the kinetic energy:

$$e_{KE} = \frac{1}{2}\,(P - P_a)\,(v_a - v). \qquad \text{(II.2.2)}$$

[3] F.B. Porzel, "Introduction to a Unified Theory of Explosions (UTE)," NOLTR 72-209, Sept.,1972

The remaining trapezoidal area is the internal energy:

$$e_I = \frac{1}{2} (P + P_a) (v_a - v). \qquad \text{(II.2.3)}$$

The area between the adiabat and the straight line connecting Pv and ambient is the waste heat. At an infinite distance from the source of the blast all of the prompt energy has been converted to waste heat.

We can estimate the ratio of the production of waste heat to the total energy using the Rankine-Hugoniot relations for changes across a shock wave:

$$\frac{e_I}{e_T} = \frac{\frac{1}{2} (P + P_a) (v_a - v)}{P (v_a - v)} = \frac{P + P_a}{2 P}.$$

For $P \gg P_a$ the internal energy is approximately 1/2 the total; hence, half the energy is subject to waste (the kinetic energy is not subject to waste). In the acoustic approximation, $P \sim P_a$ and all the energy is wasted.

In the following, two problems are addressed:

a) properties of the spherical blast wave, and

b) modifications to include the effect of the high directionality of the exiting gases.

II.2.a The Unified Theory of Explosions

The shock expansion process is adiabatic; hence, in general we can write

$$e_T = W + e_{KE} + Q \qquad \text{(II.2.4)}$$

where W is the pressure volume energy, $W = \int P dv$, e_{KE} is the kinetic energy per unit mass and Q is the specific waste heat.

The total prompt energy, the integral of the prompt energy, is defined by

$$Y(R) = 4 \Pi \int_0^R (W + e_{KE})\ r^2\ dr. \qquad \text{(II.2.5)}$$

Subject to the boundary conditions:

a) at R = Ro, the initial charge radius, Y is the hydrodynamic yield, and

b) as R approaches infinity the shock wave must completely dissipate,

the expression for the total prompt energy becomes

$$Y(R) = 4 \Pi \int_R^\infty Q\ r^2\ dr. \qquad \text{(II.2.6)}$$

The abstraction which makes UTE tractable is the QZQ hypothesis which states:

$$Q\ Z^q = \text{constant}, \qquad \text{(II.2.7)}$$

where Z is a mass corrected radius and q is a constant (which has values of 3.5 in the strong shock regime and 4.0 in the weak). Specification of a relation between R and the mass corrected radius

permits a closed form integration of Equation (II.2.6). The proof of Equation (II.2.7) is involved and will not be presented here. The reader is referred to either [1] or [3].

The concept of a mass correction to the radius was originally introduced to permit analysis of entirely different blast wave sources -- the "massless" nuclear and the standard TNT charge. The relation between the two radii is simply

$$Z = (R^3 + M)^{\frac{1}{3}} \qquad \text{(II.2.8)}$$

where M represents (essentially) the ratio of the energy in the mass to the energy in the air contained within the shock boundary.

The only remaining piece of information necessary for solution of the blast wave properties is determination of the constant in Equation (II.2.7). This is found by specifying the pressure at the transition point between the strong and weak shock regimes. In this analysis we have selected a pressure ratio of 2 since this is approximately the point at which the negative phase develops.[3] Using this value we can solve Equation (II.2.7) and (II.2.8) to determine the mass corrected transition radius and finally determine the constant via

$$Q\, Z^q = \text{constant} = Q_t\, Z_t^q.$$

The computational loop is closed by determining the area between the Hugoniot and the straight line (the waste heat in Figure 4). It is found to be

$$Q^* = \frac{\rho_a}{P_a} Q = \frac{1}{\gamma - 1}\left[\frac{\rho_a}{\rho}\left(\frac{P}{P_a}\right)^{\frac{1}{\gamma}} - 1\right] \qquad \text{(II.2.9)}$$

where the density ratio is obtained from the Rankine-Hugoniot relations:

$$D = \frac{\rho}{\rho_a} = \frac{\frac{\gamma+1}{\gamma-1} P_r + 1}{P_r + \frac{\gamma+1}{\gamma-1}} \qquad \text{(II.2.10)}$$

II.2.b Asymmetric Blast Effects

Experimental measurements of the blast fields produced by guns have shown that for a fixed distance from the observer to the muzzle, considerably larger overpressures occur in the region forward of the muzzle than in the region behind the muzzle. This is analogous to the moving charge effect which has been studied by Armendt and Sperrazza [4]. They found that the blast from a moving charge remained essentially spherical about an origin which moved with the center of mass of the decelerating charge. The deceleration of the charge could be determined by conservation of momentum. The center of mass decelerates rapidly as the expanding shock wave engulfs an ever-growing mass of initially stationary air.

Detailed calculations were made based on this effect and while it predicts higher overpressures forward of the muzzle than aft, the effect is too small to explain the order of magnitude differences which are observed in the muzzle blast experiments. This is due, primarily, to the rapid deceleration of the center of mass which is produced by a rapidly expanding spherical shock.

Porzel [3] described a concept called generalized divergence (GDV) which permits an extension of UTE to non-spherical geometries. He notes that the physical significance of the spatial coordinate in the hydrodynamic equations is a radius of curvature rather than the location relative to some earlier position. It is the local radius of curvature of the wave front which determines its divergence. Thus it is the initial shape of the charge which determines the shape of the blast field.

---

[4] B.F. Armendt, J. Sperrazza, "Air Blast Measurements Around Moving Explosive Charges, Part III," BRL Memorandum Report No. 1019, July, 1956 (AD #114950)

The initial charge for a gun muzzle blast is the barrel gases which exit when the projectile leaves the muzzle. The high overpressure of these gases causes a "barrel shock" system to form as shown schematically in Figure 5. This provides an initial source for the blast field which is far from spherical. The local radius of curvature is much greater in the forward portion of the shock system, resulting in a smaller divergence and less rapid decrease in the blast overpressure forward of the gun muzzle compared to the rear where the radius of curvature is much smaller.

The concept of GDV was incorporated into the scaling of blast overpressure provided by the QZQ hypothesis by modifying the distance scale at each angular position in the blast field to correct for the initial non-spherical geometry. The value of R used in the QZQ calculation was given by

$$R = \frac{R(\theta)}{G(\theta)} \qquad \text{(II.2.11)}$$

where $G(\theta)$ is a geometry factor which was determined on an ad hoc basis. It was found that the experimental data were reasonably well represented using a geometry factor given by

$$G(\theta) = \frac{3}{4}\left[\cos\theta + \sqrt{\cos^2\theta + (4/3)^2}\right] \qquad \text{(II.2.12)}$$

The derivation of this function was based on a velocity argument and is given in Appendix A.

II.3 Pulse Length Calculations

In Part 1 the pulse length of the overpressure pulse was determined based on a characteristic length and the particle velocity. The characteristic length was representative of the volume occupied by the remaining prompt energy in the blast.

An alternative method of calculating the pulse length has been

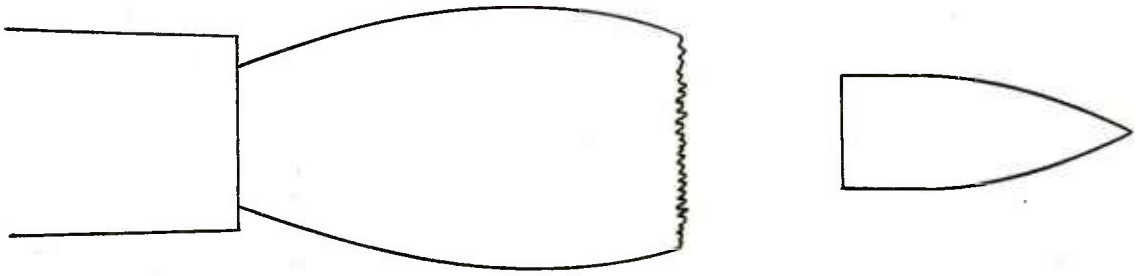

FIGURE 5. "Barrel Shock" Produced by Propellent Gases Exiting Muzzle.

developed based on the propagation of waves of finite amplitude. As the blast wave from the explosion expands, the initial high overpressure at the shock front decreases behind the shock front. At some point during the expansion the overpressure behind the shock drops to zero and upon further expansion the blast wave develops a negative phase.[5] The radius at which the overpressure first drops to zero is called the transitions radius. The fluid velocity behind the shock has a similar behavior with a large velocity in the direction of the shock velocity decreasing to zero and becoming negative. The resulting pulse forms are shown in Figure 6. These pulses of finite amplitude propagate into the undisturbed air. The propagation velocity is not the same for all portions of the pulse, but depends on the local speed of sound and the fluid velocity. The leading edge of the pulse propagates with a greater velocity than the rest of the pulse and therefore the pulse increases in length as it propagates outward.

The local wave speed for the pulse of finite amplitude is given by [6]

$$c = a_n + u \qquad \text{(II.3.1)}$$

where a_n and u are the local value of the speed of sound and fluid velocity. For an isentropic process the local wave speed becomes

$$c = a + \frac{\gamma+1}{2} u \qquad \text{(II.3.2)}$$

where a is the speed of sound in the undisturbed region ahead of the pulse. The propagation of a shock is not an isentropic process, but for overpressures at distances greater than the transition radius the corrections are small compared to the uncertainty in the measured values of pulse length.

The trajectories of the pulse front and the point at which the fluid velocity drops to zero are shown in Figure 7. The pulse shape is shown at the transition radius R_t and at two other positions.

We will define the pulse length τ as the time between these two trajectories at a given position R. Note that as the shock wave

[5] Yu.B. Zel'dovich, Yu.P. Raizer, Physics of Shock Waves and High Temperature Hydrodynamic Phenomena, Vol. 1, Academic Press, New York, 1966.

[6] H.W. Liepmann, A. Roshko, Elements of Gasdynamics, John Wiley & Sons, New York, 1957.

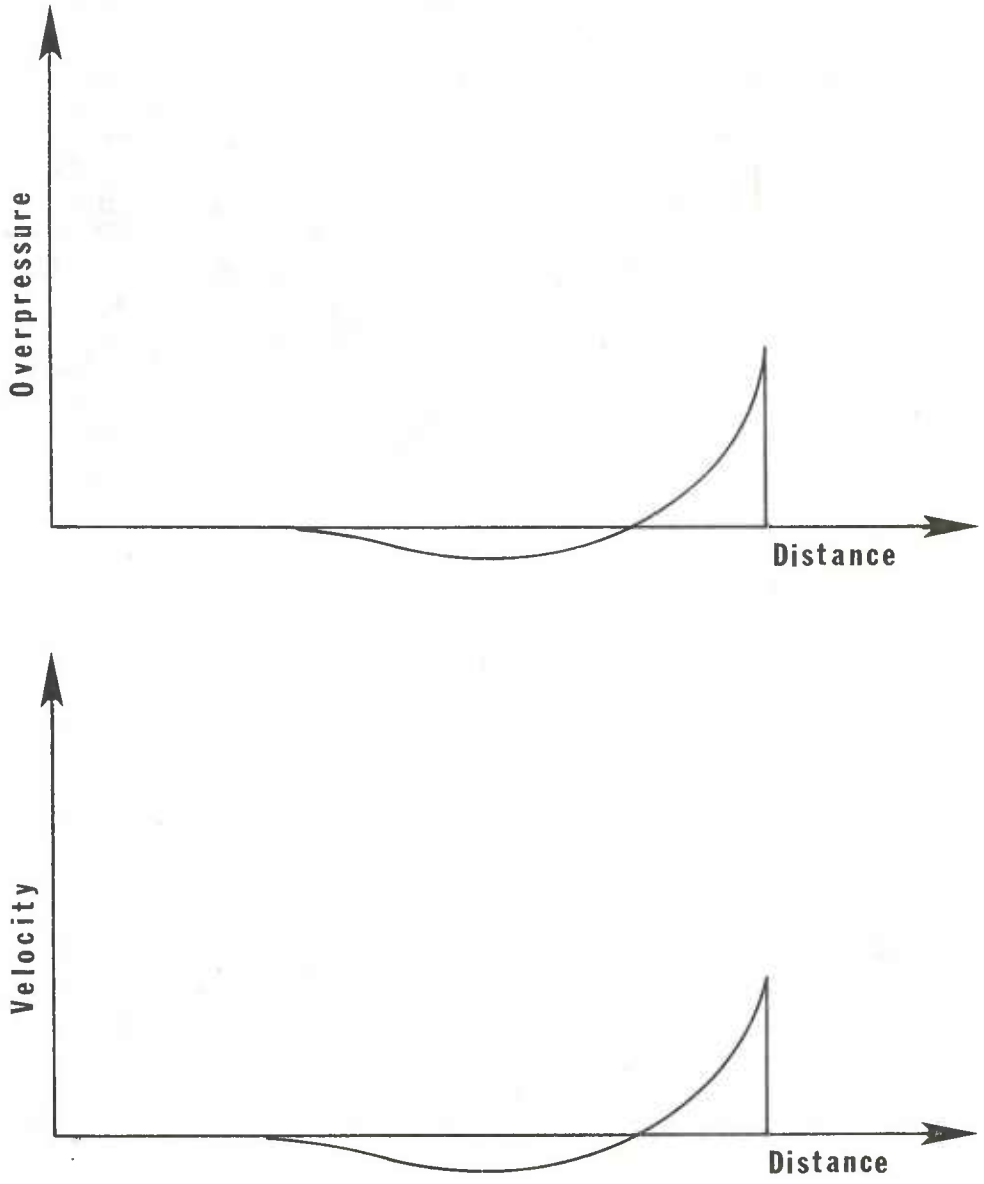

FIGURE 6. Sketch of Overpressure and Fluid Velocity in the Blast Pulse After the Negative Phase Has Developed.

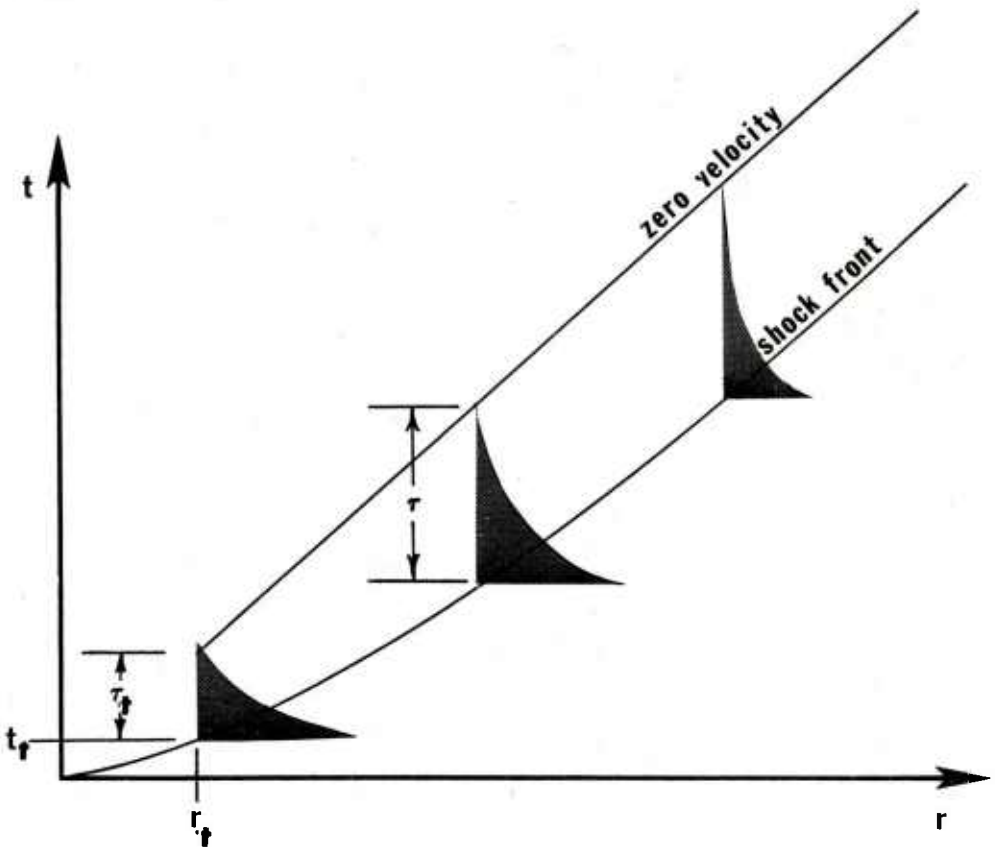

FIGURE 7. Sketch of the Trajectories of the Pulse Front and the Point Where Fluid Velocity Drops to Zero.

expands and the fluid velocity behind the shock approaches zero, the shock front approaches the speed of sound and the pulse length approaches an asymptotic value which then propagates as an acoustic wave.

The zero-velocity trajectory is given by

$$t_1 = \frac{1}{a}(R - R_t) + t_t + \tau_t \qquad \text{(II.3.3)}$$

and the shock front velocity by

$$t_2 = \frac{1}{a}\int_{R_t}^{R} \frac{dx}{1 + \frac{\gamma+1}{2}\frac{u}{a}} + t_t. \qquad \text{(II.3.4)}$$

The difference of these expressions gives the pulse length

$$\tau = \tau_t + \frac{1}{a}(R-R_t) - \int_{R_t}^{R} \frac{dx}{1 + \frac{\gamma+1}{2}\frac{u}{a}} \qquad \text{(II.3.5)}$$

where τ_t is the initial pulse length at the transition radius R_t. The initial pulse length τ_t can be estimated with the aid of Figure 8 which shows the overpressure at the time t when the shock reaches the transition radius.[7] This is the radius for which the negative phase has fully developed and occurs at a pressure ratio of two across the

[7] H.L. Brode, "Numerical Solutions of Spherical Blast Waves," J. Appl. Phys., Vol. 26, No. 6, June, 1955, pp. 766-775

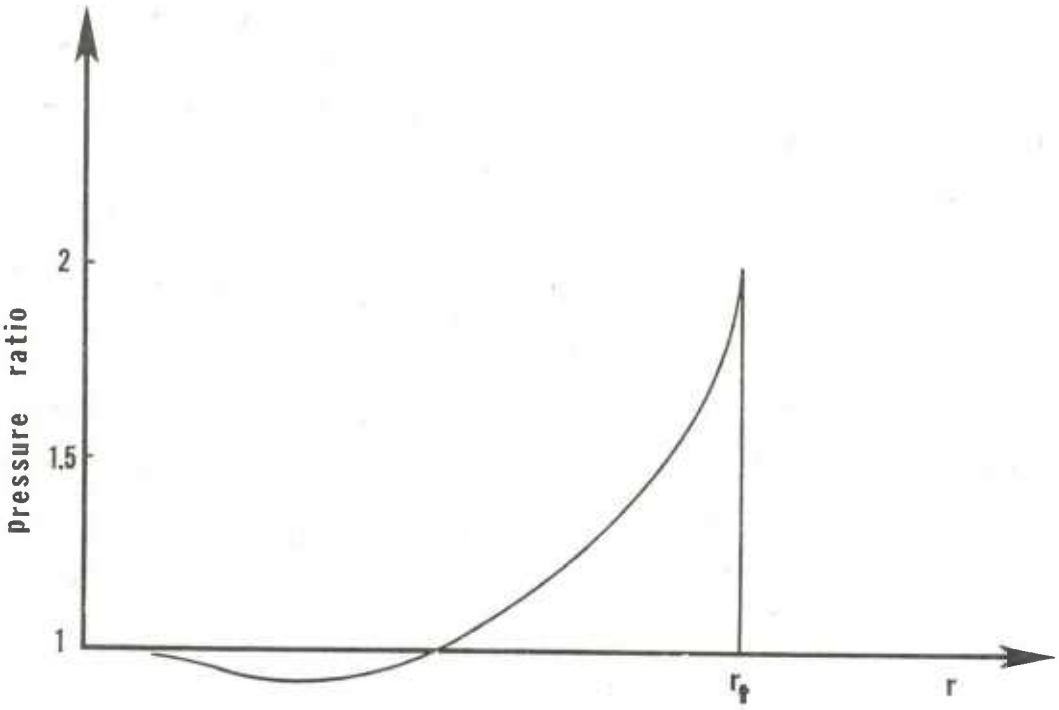

FIGURE 8. Overpressure Pulse at Transition. The Pressure Ratio Drops to Unity of Approximately One-Half the Transition Radius r_t.

shock. If we make the ad hoc assumption that the pulse occupies half the spherical radius at transition then the characteristic initial pulse length is given by

$$\tau_t = \frac{R_t}{2c_s} \qquad \text{(II.3.6)}$$

where c_s is the wave speed of the shock at a pressure ratio of two.

The pulse length is calculated from Equation (II.3.5) using the initial pulse length given in Equation (II.3.6) and the fluid velocity determined from the Rankine-Hugoniot relations and the local value of overpressure determined from UTE.

III. Results

The purpose of this study was to determine the applicability of the theory presented in Part I for smaller caliber guns and to extend the analysis to include those positions aft of the muzzle exit plane.

III.1 Guns Considered

The above theories were applied to six different guns and to one case where the propellent mass and specific energy were changed (zone 5 vs. zone 8). The guns and their characteristics are listed in Table 1. [8][9] The barrel diameters range from the .30 caliber pistol/rifle to an 8 inch naval gun.

The .30 caliber pistol was (apparently) a shortened .30 caliber rifle. All of the physical characteristics are the same, the different projectile muzzle velocity being obtained from a different propellant loading. The two cases using the 105 mm Howitzer provide an excellent evaluation of the effect of muzzle velocity on the initial yield.

[8] P.S. Westine, J.C. Hokanson, "Prediction of Stand-off Distances to Prevent Loss of Hearing from Muzzle Blast," Southwest Res. Inst. Report No. R-CR-75-003, Feb., 1975 (AD A005274).
[9] P.S. Westine, "Modeling the Blast Field Around Naval Guns and Conceptual Design of a Model Gun Blast Facility," Southwest Res. Inst. Report No. TR 02-2643-01, Sept., 1970 (AD 875984).

Table 1. Characteristics of guns

Characteristics	20 mm Gun	.30 cal Rifle	.30 cal Pistol	3 inch Gun	105 mm Howitzer	105 mm Howitzer	8" Naval Gun
Barrel Diameter (m)	.020	.00762	.00762	.0762	.105	.105	.204
Length (m)	1.357	.5588	.23	3.81	3.55	3.55	8.95
Rifling Height (mm)	.157	.102	.102	1.6	3.5	3.5	4.2
Projectile Mass (kg)	.1212	.0097	.0097	5.9	14.96	14.96	151.9
Vel. (m/s)	859	837	446	805	332	650	758.3
Propellent Mass (kg)	.028	.0028	.00084	1.84	.626	2	44.52
Specific Energy (Mj/kg)	3.468	3.606	5.05	3.14	2.93	4.07	2.742

All the chamber pressure ratios were assumed approximately 3000 -- the results are very insensitive to this parameter.

III.2 Comparison of Theory and Experiment

The predictions of the theory have been compared to these data and the results are presented in Figures 9 through 13. The theory is clearly capable of predicting the muzzle blast overpressure for guns of vastly different calibers. Careful examination of the curves shows that the theory will also predict the angular variations in the blast field with reasonable accuracy over the full range of calibers examined. The largest discrepency between theory and experiment occurs at distances beyond 50 calibers where the experimental data exceeds the theoretical predictions. The experimental data were all obtained with the guns firing essentially horizontally over the ground or a ground plane. The shock wave associated with the muzzle blast will reflect from this plane causing a reinforcement to the primary shock which increases the measured overpressure. Indeed, in much of the data the measured overpressure values increase with increasing distance from the muzzle for distances beyond 50 calibers. Since the theory does not account for reflected shocks the disagreement at large distances is not surprising.

Examination of the angular behavior of the theory for distances less than 50 calibers for the cases considered reveals that on the average the theoretical predictions tend to overestimate the overpressure in the aft (greater than 90 degrees) portion of the blast field and underestimate the overpressure in the forward portion of the field. This is particularly noticeable for the .30 caliber pistol, the smallest gun considered. This effect is a result of the particular form of the geometry factor chosen. An improvement might be obtained by modifying the form of the geometry factor according to the ratio of random to ordered motion in the muzzle gases as proposed in Part I.

Since the current theory contains the kinetic energy of the muzzle gas in the prompt energy the overpressure was calculated for a 105 mm howitzer in which the muzzle velocity varied as a result of different propellent charges. The results are shown in Figure 14. The theory accurately predicts muzzle blast overpressure for these cases although the muzzle velocity is higher by a factor of two for the zone 8 (Z8) compared to the zone 5 (Z5) experiment. The result shows that the theory will predict the muzzle blast from guns over a considerable range of muzzle velocity.

Pulse length of the overpressure pulse is more difficult to compare since there are large variations in the experimental values obtained. A typical situation is shown in Figure 15 for the case of the same 20 mm gun shown in Figure 12. The theory predicts that the pulse length will increase with distance from the muzzle until it reaches some asymptotic value but the experiments often show that the pulse length first increases then decreases with distance. This

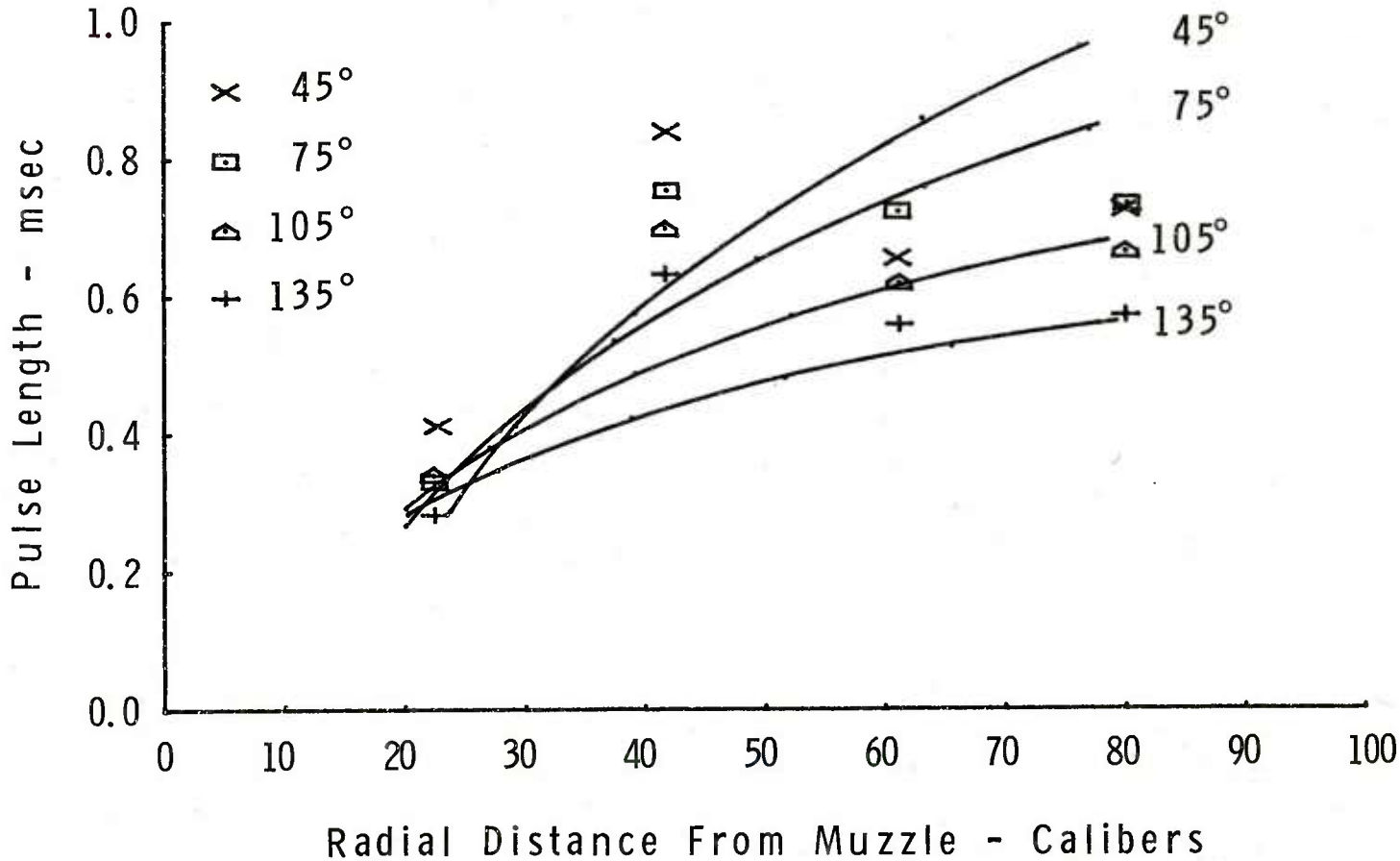

FIGURE 15. Overpressure Pulse Length from 20 mm Gun.

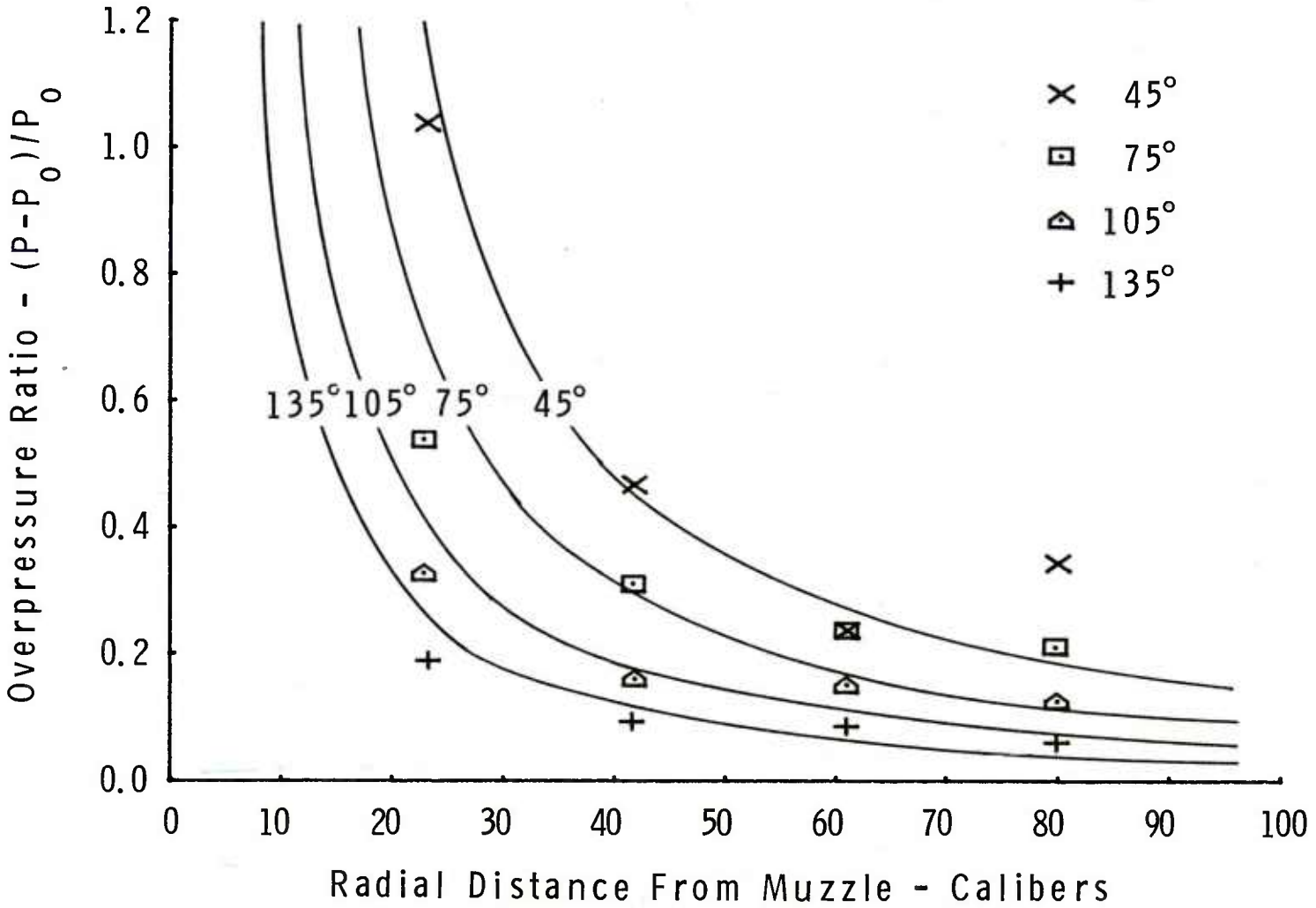

FIGURE 9. Overpressure from 8 inch Naval Gun.

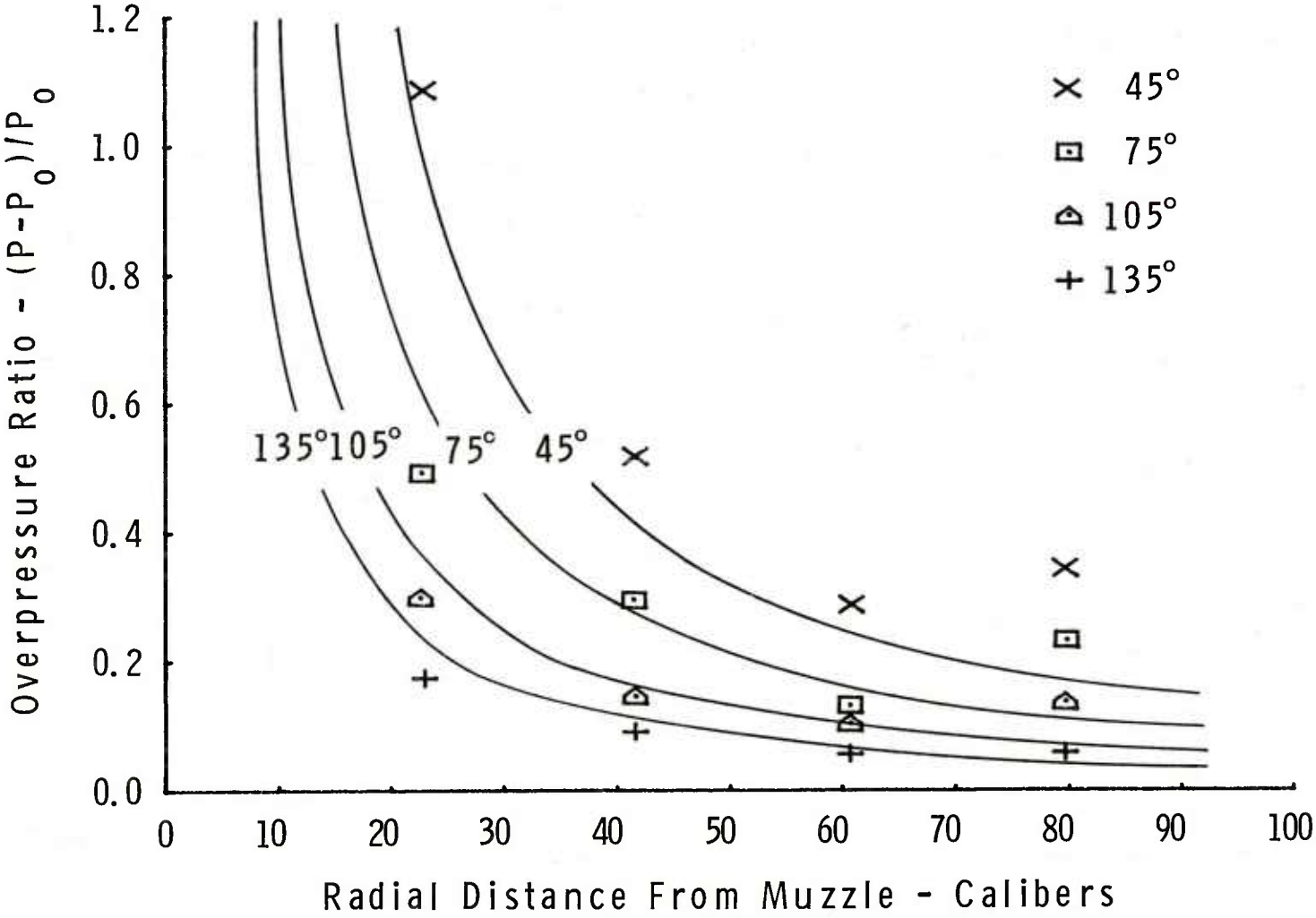

FIGURE 10. Overpressure from 3 inch Naval Gun.

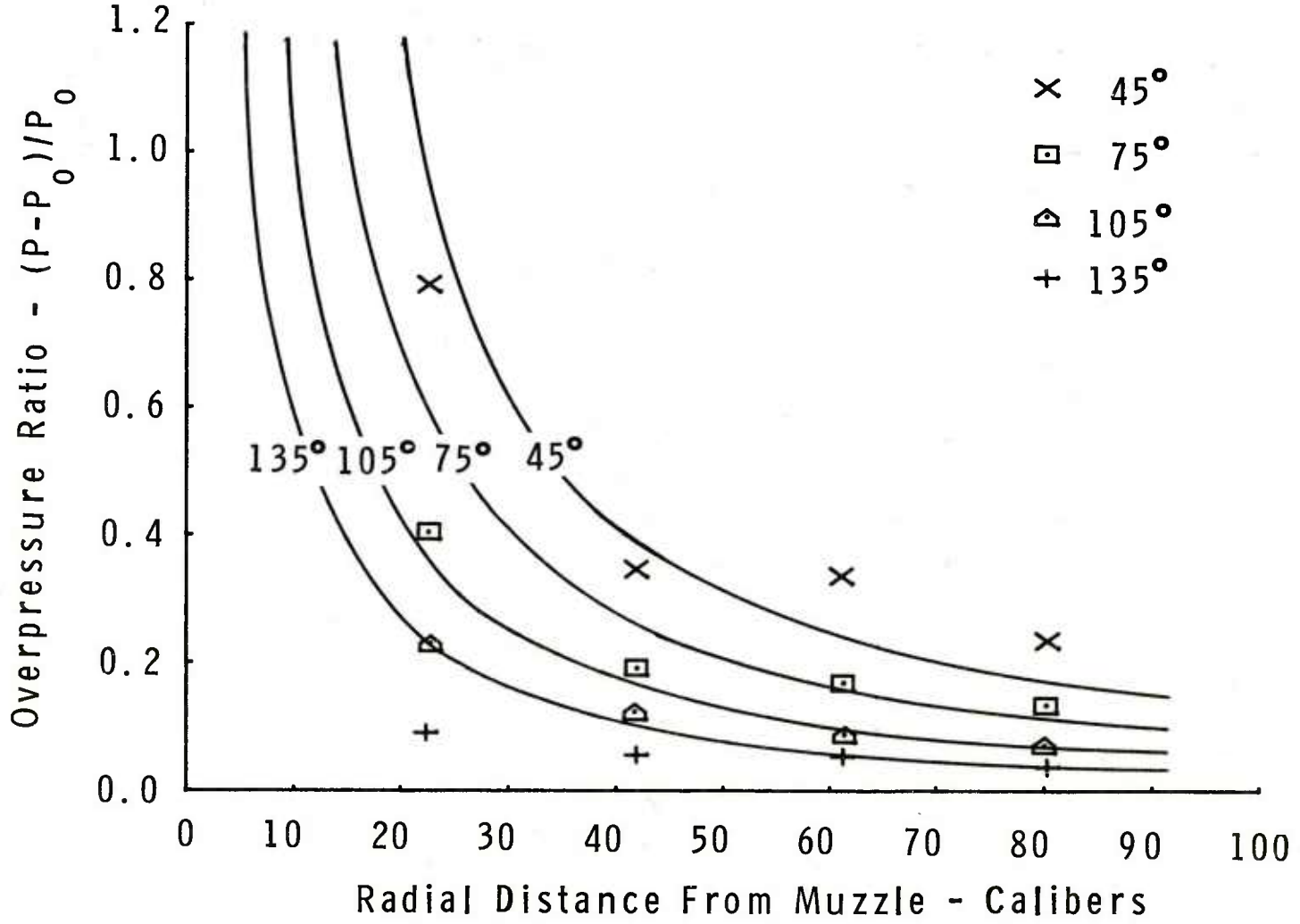

FIGURE 11. Overpressure from 20mm Gun

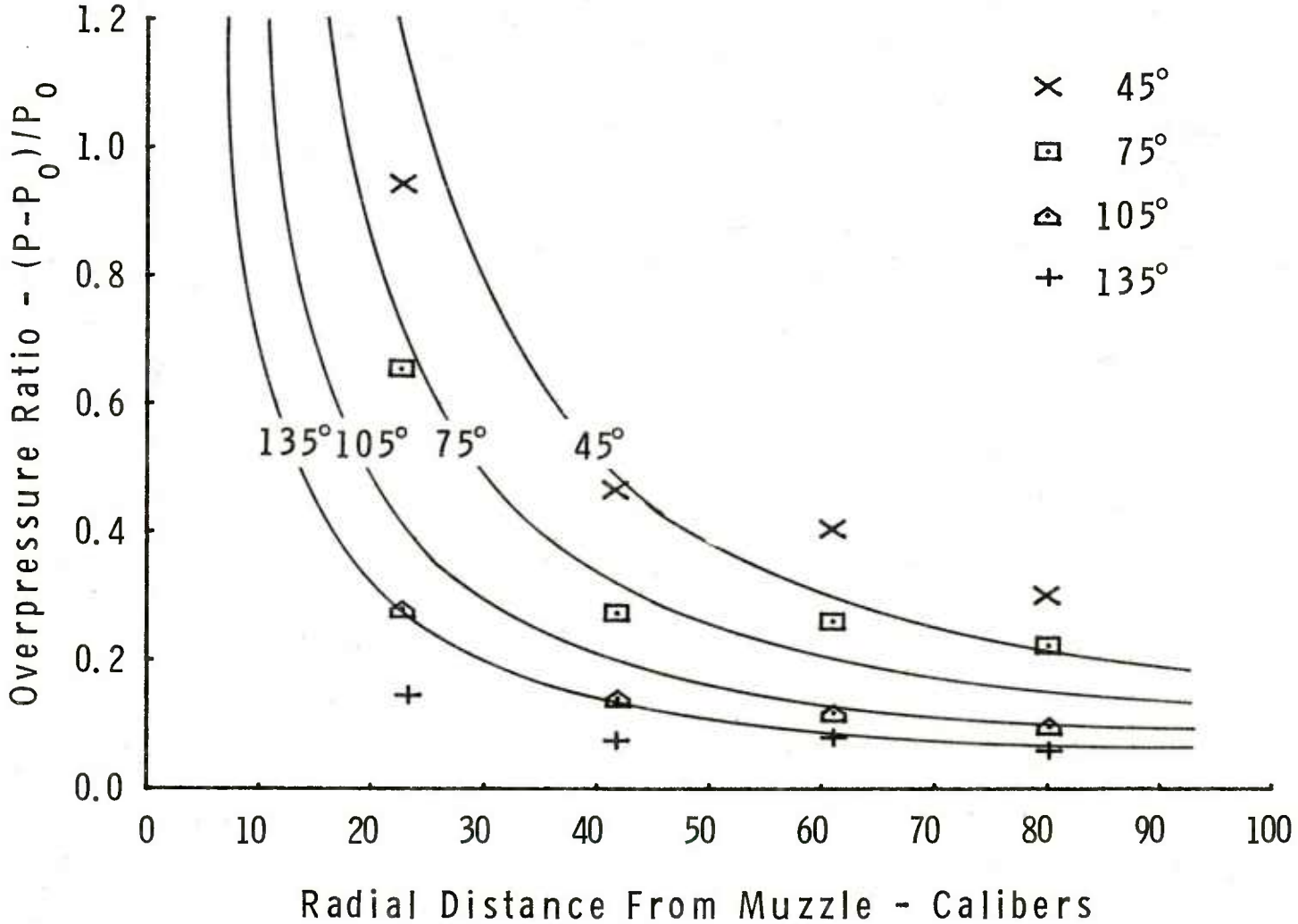

FIGURE 12. Overpressure from .30 Caliber Rifle.

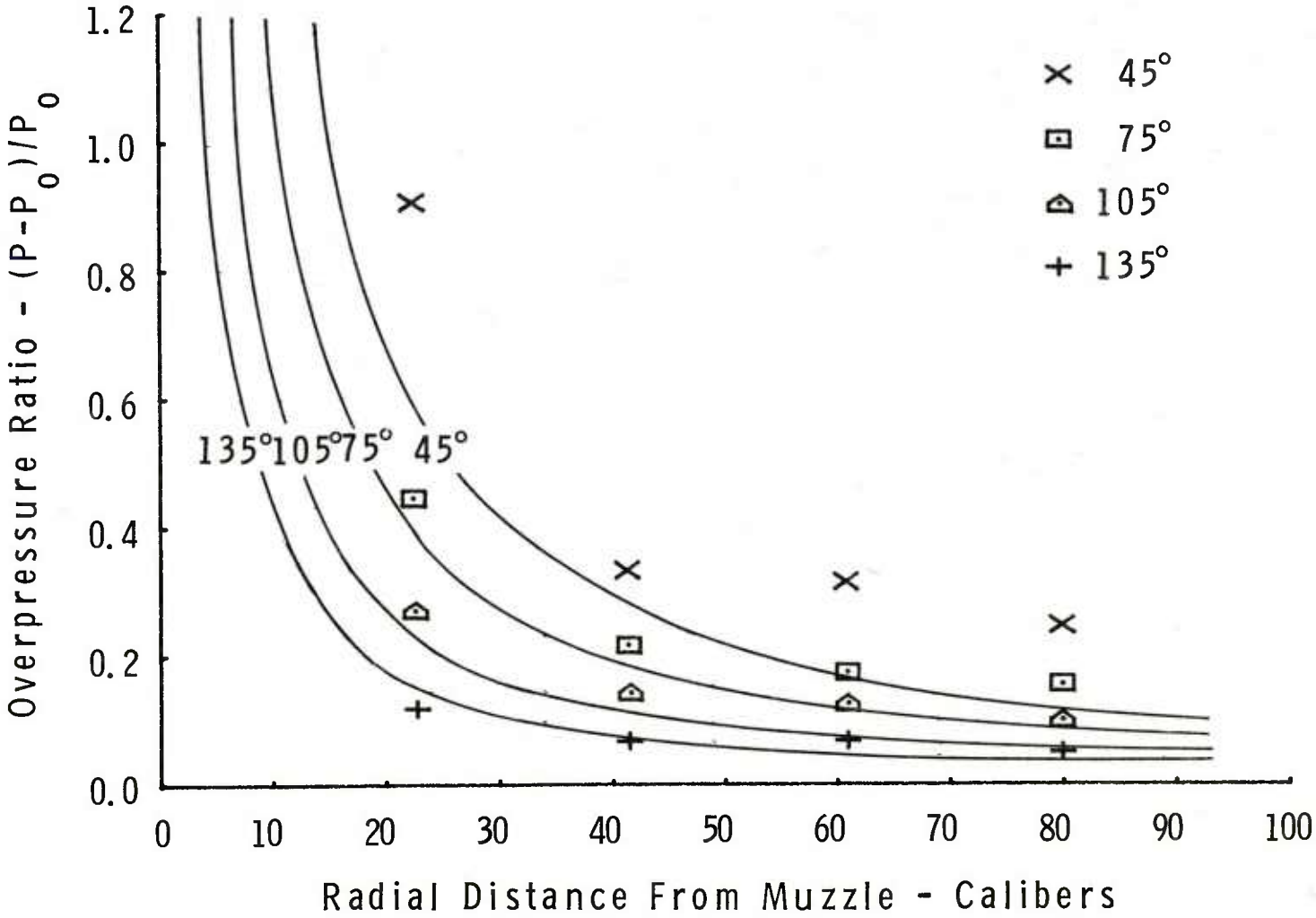

FIGURE 13. Overpressure from .30 Caliber Pistol.

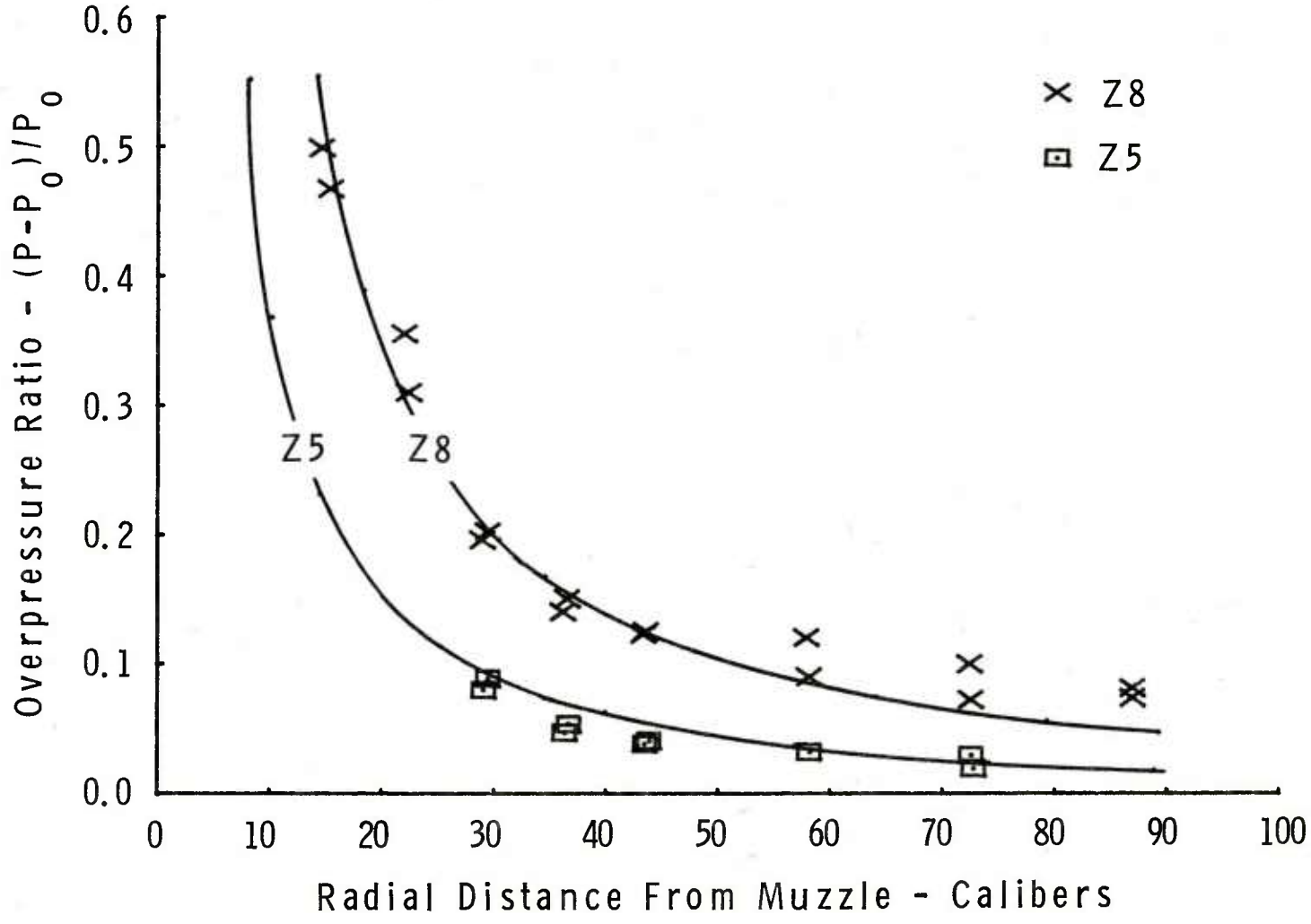

FIGURE 14. Overpressure from 105 mm Howitzer at Two Muzzle Velocities. Z8 is 650 m/s and Z5 is 332 m/s.

decrease first appears at distances greater than 50 calibers and may be related to the shock reflection from the ground plane which produces pulses of complex shape.

Predicted pulse lengths for four guns ranging from an 8 inch naval gun to a .30 caliber rifle are shown in Figure 16. The pulse length was calculated for an angle of 90 degees to the line of fire and the experimental data were taken at 75 and 105 degrees. The measured values of the pulse length are reasonably well predicted by the theory over the wide range of pulse lengths produced by guns of greatly different caliber.

These results indicate that the theory gives reasonable agreement with experiment over a wide range of gun calibers. The theory has the advantage of simplicity and ease of calculation and should be of great value in the prediction of free-field gun muzzle blast effects.

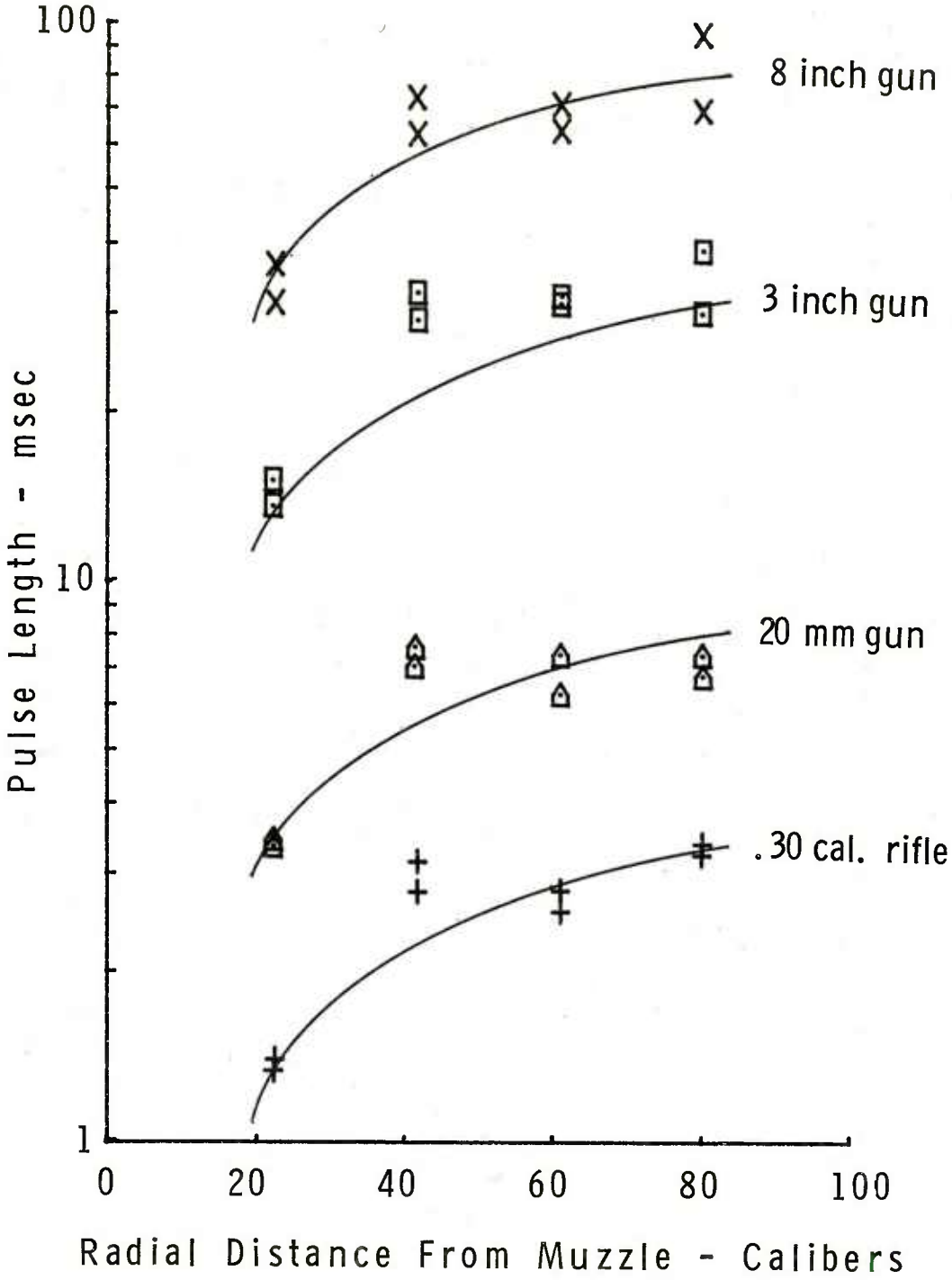

FIGURE 16. Overpressure Pulse Length for Four Guns.

REFERENCES

[1] B. Henriksen, B. Cummings,"A Predictive Scheme for the Blast Environment of Army Weapons, Part I. Devlopment and Validation of the Theory," BRL Technical Report ARBRL-TR-02044, Feb. 1978. (AD #A053487)

[2] F.B. Porzel, "Study of Shock Impedance Effects in a Rough Walled Tunnel," IDA Log No. HQ 68-7324, Mar., 1969 (AD 684790).

[3] F.B. Porzel, "Introduction to a Unified Theory of Explosions (UTE)," NOLTR 72-209, Sept.,1972.

[4] B.F. Armendt, J. Sperrazza, "Air Blast Measurements Around Moving Explosive Charges, Part III," BRL Memorandum Report No. 1019, July, 1956. (AD #114950)

[5] Yu.B. Zel'dovich, Yu.P. Raizer, Physics of Shock Waves and High Temperature Hydrodynamic Phenomena, Vol. 1, Academic Press, New York, 1966.

[6] H.W. Liepmann, A. Roshko, Elements of Gasdynamics, John Wiley & Sons, New York, 1957.

[7] H.L. Brode, "Numerical Solutions of Spherical Blast Waves," J. Appl. Phys., Vol. 26, No. 6, June, 1955, pp. 766-775.

[8] P.S. Westine, J.C. Hokanson, "Prediction of Stand-off Distances to Prevent Loss of Hearing from Muzzle Blast," Southwest Res. Inst. Report No. R-CR-75-003, Feb., 1975 (AD A005274).

[9] P.S. Westine, "Modeling the Blast Field Around Naval Guns and Conceptual Design of a Model Gun Blast Facility," Southwest Res. Inst. Report No. TR 02-2643-01, Sept., 1970 (AD 875984).

APPENDIX

The form of the geometry function $G(\theta)$ was developed on the basis of a moving charge. If the velocity at some point in the blast field is the sum of the charge velocty V_c and the blast velocity for a stationary charge V_s then $V = V_c + V_s$ is assumed to be in the direction of the radius vector from the muzzle. If the field position is determined by the distance from the muzzle and the polar angle relative to the line of fire then θ is the angle between V and V_c and

$$V_s^2 + V^2 + V_c^2 - 2VV_c\cos\theta \tag{A1}$$

or

$$\left(\frac{V}{V_s}\right)^2 - 2\frac{V}{V_s}\frac{V_c}{V_s}\cos\theta + \left(\frac{V_c}{V_s}\right)^2 - 1 = 0. \tag{A2}$$

Solving for the ratio V/V_s we obtain

$$\frac{V}{V_s} = \frac{V_c}{V_s}\left\{\cos\theta \pm \sqrt{\cos^2\theta - \left[1 - \left(\frac{V_s}{V_c}\right)^2\right]}\right\} \tag{A3}$$

We assume that the geometry factor has a similar form, i.e.,

$$G(\theta) = \alpha\left(\cos\theta + \sqrt{\cos^2\theta + \beta^2}\right) \tag{A4}$$

where α and β are constants to be determined.

If we require that at an angle of 90 degrees from the barrel axis the geometry factor have the value unity, then

$$\beta = 1/\alpha$$

In Part 1 [1] we found that the kinetic energy of ordered motion at the muzzle was approximately twice that of random motion. Based on this result we require

$$G(0) = 2. \tag{A6}$$

This gives the results

$$\alpha = \frac{3}{4} \tag{A7}$$

and

$$G(\theta) = \frac{3}{4}\left[\cos\theta + \sqrt{\cos^2\theta + \frac{16}{9}}\right] . \tag{A8}$$

BASIC PROGRAM

A BASIC computer program has been constructed to perform the calculations for the muzzle blast field based on the preceding analysis. The program is listed at the end of this section. The input parameters required for the program are as follows:

1. Projectile mass - kilograms (kg)
2. Muzzle velocity - metres/second (m/s)
3. Propellant specific energy - joules/kilogram (j/kg)
4. Ratio of peak chamber pressure to ambient - dimensionless
5. Barrel length - metres (m)
6. Barrel diameter - metres (m)
7. Height of barrel rifling - metres (m)

When execution of the program begins the program will pause for input until these values are entered in the order given above. When the last value is entered the program calculates the overpressure at the choke position and at the muzzle and an equivalent explosive yield. Next, the program will pause to allow optional values of Q1, Q2 and the ratio of specific heats to be entered if desired. The variables Q1 and Q2 are the exponents in the Porzel QZQ hypothesis for the strong and weak shock regimes and have the standard values of 3.25 and 3.5 respectively. The standard value of gamma is 1.4. After the option is exercised the program computes the transition radius and pauses until the desired angular position in the blast field is entered. This is the angle measured from the line of fire to the radius vector from the muzzle to the field location and lies between 0 and 180 degrees.

The program is designed to calculate overpressure and pulse length as a function of distance from the muzzle at the input angle. The program will pause until the desired distance closest to the muzzle is entered. It then pauses until an increment in the radial distance is entered and again until the total number of increments desired is entered. The program then computes the overpressure and pulse lengths at each radial location specified for the input angle. When these computations are completed the program pauses to allow the option of terminating the program or specifying another angle. If a new angle is entered then the program pauses to allow an option of continuing with the same radial locations or changing to new radial locations. When the last angular position desired has been calculated the operator enters minus one to terminate execution.

Please note that this listing is in lower case and a mix between BASIC and BASIC+. The user must change it for his particular system.

PROGRAM LISTING

```
100    for n=1 to 5 step 1
110    print
120    next n
140    print "Muzzle Blast Overpressure and Pulse Length"
150    print "----------------------------------------"
160    print
170    print
180    print
190    rem...input section
200    rem...variable definitions are as follows
201    rem...projectile:
202    rem...
203    rem...propellant:
204    rem...
205    rem...
206    rem...pressure:
207    rem...barrel
208    rem...
209    rem...
210    print "projectile","mass (kg)",,
220    input w0
225    print
230    print ,"velocity (m/sec)",
240    input v0
245    print
246    print
250    print "propellant","mass (kg)",,
260    input w1
265    print
290    print,"specific energy (j/kg)",
300    input x2
305    print
306    print
310    print "chamber pressure ratio (p/p0)",,
320    input p0
325    print
326    print
330    print "barrel","length (m)",,
340    input L0
345    print
350    print ,"diameter (m)",,
360    input d0
365    print
370    print ,"groove height (m)"
```

```
380    input L1
390    print
395    print
400    rem...    end input data
1000   rem...
1010   rem...begin energy calculations
1011   rem...
1012   rem...
1013   rem...
1020   e2 = x2*w1
1030   e1 = .5*w0*v0^2
1040   e0 = e2 - e1
1050   print
1060   print ,"   energy calculations"
1070   print
1080   print "total energy in propellant",,e2;"joules"
1090   print "kinetic energy in projectile",,e1;"joules"
1100   print "maximum available energy",,e0;"joules"
1110   p0 = p0 - 1
2000   print
2001   print ,"   interior losses"
2002   print
2010   rem... roughness factor = h, overpressure at choke = x
2020   rem... o'pressure ratio at muzzle and initial yield = y0
2021   rem... choke length = L2
2030   h = L1/d0
2040   L2 = 0
2050   x = p0
2060   rem... if choke l/d > gun then l/d assume no choke losses
2065   if h = 0 goto 2180
2070   if 15/h^.1 > (L0/d0) goto 2180
2080   L2 = 15/h^.1
2090   rem... if p0 > 100 use fitted curve
2100   if p0>100 goto 2160
2110   x = p0
2120   c = (1+x)*(1+4*x^2/5/(1+x)/(9+x))^5 - 1
2130   if abs(c-p0)<.001 goto 2170
2140   x = x - (x-1)*(c-p0)/(c-1.29)
2150   goto 2110
2160   x = exp(.9211*log(p0) - 2.138)
2170   print "overpressure ratio at";L2*d0;"m is",x;"    (choke)"
2180   y0 = exp((2*h*(L2-L0/d0)+1.068*log(x))/1.068)
2190   print "overpressure at";L0;" m is",,y0;"  muzzle"
2200   f = p0/y0
2210   rem... reduction in e(avail)
2220   y0 = e0/(6*f)
2230   e3 = w1/12*v0^2
2231   y0 = y0 + e3
2232   print
2233   print ,"   equivalent explosion parameters"
```

```
2234   print
2240   print "yield",,,y0;" joules"
2250   r0 = d0
2251   m0 = w1/6
2252   for m = 1 to 5 step 1
2253   print
2254   next m
2260   print "for optional q1, q2, gamma enter one; std. values enter 0"
2261   input o1
2262   if o1 = 0 goto 2280
2270   print "enter q1"
2271   input q1
2272   print "enter q2"
2273   input q2
2274   print "enter ratio of specific heats, gamma"
2275   input g
2276   goto 2300
2280   q1 = 3.25
2281   q2 = 3.5
2282   g = 1.4
2300   rem... q0 = pressure/density (atmospheric)
2301   q0 = 78340
2302   h = .25
2303   q5 = 1889
2304   p0 = 101325
2305   d = 1.293
2310   m = m0*h/5.416
2320   z0 = (r0^3 + m)^(1/3)
2400   rem... find transition radius
2420   a1 = (q1-q2)/(3-q2)
2430   a2 = (q1-3)*y0/(12.566*q5*z0^3)
2440   if q1=q2 goto 2480
2450   z = 1
2451   s = z
2452   f = a1*s^3 - s^q1 + a2
2453   f1 = 3*a1*s^2 - q1*s^(q1-1)
2454   z = z - f/f1
2455   if abs (z-s) < .001 goto 2460
2456   goto 2451
2460   z1 = z
2461   goto 2481
2480   z1 = a2^(1/q1)
2481   r2 = ((z1*z0)^3 - m)^(1/3)
2482   print "transition radius",r2,"metres"
2500   rem... set up qzq constants a and b
2510   a = q5/q0*(z1^q1)
2520   b = q5/q0*(z1^q2)
2530   print
2540   print
2600   rem... set up desired radial locations
```

```
2601   print "input angle (degrees)"
2602   input t1
2603   let t2=cos(t1*pi/180)
2604    r8=.75*(t2 + sqr(t2^2+16/9))
2606   print "enter initial radius (metres)"
2607   input r3
2610   print "input radial increment (metres)"
2611   input r4
2620   print "input number of increments desired"
2621   input k
2622   print "radius","overpressure","pulse length"
2623   print "(metres)","(p-p0)/p0","(seconds)"
2624   print "********","**********","**********"
2625   s1 = 0
2626   c0 = sqr(g*p0/d)
2627   t5 = r2*r8/1000
2630   for i=1 to k
2640   r = (r3+r4*(i-1))
2650   for j=1 to 10
2660   if r <= r2*r8 goto 2780
2670   if (r-r2*r8) < r4 goto 2700
2680   y2 = r4/10
2690   goto 2710
2700   y2 = (r-r2*r8)/10
2710   v = (r-(10-j)*y2)/r8
2720   gosub 4000
2730   u = (p1-1)*sqr(2*q0/((g+1)*p1+(g-1)))
2740   s1 = s1 + y2/(1+(g+1)/2*u/c0)
2750   next j
2760   t = t5 + ((r-r2*r8) - s1)/c0
2770   goto 2800
2780   t = t5
2785   v = r/r8
2790   gosub 4000
2800   p = p1-1
2810   print r,p,t
2820   goto 2840
2830   print "error; radius",r,"less than muzzle diameter"
2840   next i
3040   print "input next angle (degrees) or -1 to terminate"
3041   input t1
3050   if t1<0 goto 3070
3051   t2 = cos(t1*pi/180)
3052   r8 = .75*(t2+sqr(t2^2+16/9))
3060   print "enter 1 to change radius; 0 to continue"
3061   input a8
3062   if a8 = 0 goto 2625
3063   goto 2606
3070   print "end of ute muzzle blast calculations"
3080   goto 9999
```

```
4000    if v<=r0 goto 2830
4010    z = ((v^3+m)^(1/3))/z0
4020    if z <= z1 goto 4060
4030    q = b/(z^q2)
4040    y1 = q0*q/(q2-3)*(z0*z)^3
4050    goto 4070
4070    rem... now calculate overpressure
4080    if q < 7.45e-7 goto 4210
4090    if q > 1.167 goto 4310
4100    p1 = 5
4110    a1 = (g+1)/(g-1) + p1
4120    a2 = (g+1)/(g-1)*p1 + 1
4130    a3 = 1+(g-1)*q
4140    f = a1*p1^(1/g) - a3*a2
4150    f1 = 1/g*a1*p1^(1/g-1) + p1^(1/g)
4160    f1 = f1 - (g+1)/(g-1)*a3
4170    n = f/f1
4180    if abs(n) < .001 goto 4340
4190    p1 = p1-n
4200    goto 4110
4210    p=.02
4220    c1 = 24*q*g^3/(g+1)
4230    f = 3*p^4 - 2*p^3 + c1
4240    f1 = 12*p^3 - 6*p^2
4250    n = f/f1
4260    if abs(n) < .0005 goto 4290
4270    p = p-n
4280    goto 4230
4290    p1 = p+1
4300    goto 4340
4310    k1 = 22+16*log(q)/2.303
4320    l = 11.5 - sqr(132.25 - k1)
4330    p1 = 10^l + 1
4340    return
9999    end
```

DISTRIBUTION LIST

No. of Copies	Organization
12	Commander Defense Documentation Center ATTN: DDC-TCA Cameron Station Alexandria, VA 22314
3	Director Defense Advanced Research Projects Agency ATTN: Tech Lib NMRO PMO 1400 Wilson Boulevard Arlington, VA 22209
5	Director of Defense Research & Engineering ATTN: DD/TWP DD/S&SS DD/T&SS AD/SW Mr. J. Persh, Staff Specialist Materials and Structures Washington, DC 20301
1	Director Institute for Defense Analysis ATTN: IDA Librarian, Ruth S. Smith 400 Army Navy Drive Arlington, VA 22202
2	Assistant to the Secretary of Defense (Atomic Energy) ATTN: Document Control Donald R. Cotter Washington, DC 20301
4	Director Defense Intelligence Agency ATTN: DT-1B DB-4C RDS-3A4 DT-2/Wpns & Sys Div Washington, DC 20301
6	Director Defense Nuclear Agency ATTN: SPTD, Mr. J. Kelso SPSS, Dr. E. Sevin SPAS, Mr. J. Moulton STSP STVL, Dr. Lavier RATN, CDR Alderson Washington, DC 20305
6	Director Defense Nuclear Agency ATTN: DDST, Mr. P. Hass DDST, Mr. M. Atkins STTL, Tech Lib (2 cys) STSI, Archives SPSS, LT J.T. Williams Washington, DC 20305
1	Commander Field Command, DNA ATTN: FCPR Kirtland AFB, NM 87115
1	Commander Field Command, DNA Livermore Branch ATTN: FCPRL P. O. Box 808 Livermore, CA 94550
1	Director Defense Communications Agency ATTN: NMCSSC (Code 510) Washington, DC 20305
1	Director Joint Strategic Target Planning Staff JCS ATTN: Sci & Tech Info Lib Offutt AFB Omaha, NB 68113

DISTRIBUTION LIST

No. of Copies	Organization
2	Director National Security Agency ATTN: E. F. Butala, R154 P. E. Deboy, NSA 5232 Ft. George G. Meade, MD 20755
1	Commander US Army Materiel Development and Readiness Command ATTN: DRCDMD-ST, N. Klein 5001 Eisenhower Avenue Alexandria, VA 22333
9	Commander US Army Aviation Research and Development Command ATTN: DRSAV-E AAH-PM, BG E.M. Browne W.H. Brabson M. Corgiatt ASE-PM COBRA-PM Blackhawk-PM DRDAV-EQ, C. Crawford DRDAV-EQA, R. Wolfe 12th and Spruce Streets St. Louis, MO 63166
1	Director US Army Air Mobility Research and Development Command ATTN: W. Andre Ames Research Center Moffett Field, CA 94035
4	Commander US Army Electronics Research and Development Command Technical Support Activity ATTN: DELSD-L DELSD-TL-IR R. Freiberg J. Roma A. Sigismondi Fort Monmouth, NJ 07703
1	Commander US Army Communications Rsch and Development Command ATTN: DRDCO-PPA-SA Fort Monmouth, NJ 07703
1	Commander US Army Missile Research and Development Command ATTN: DRDMI-R Redstone Arsenal, AL 35809
1	Commander US Army Missile Materiel Readiness Command ATTN: DRSMI-AOM Redstone Arsenal, AL 35809
1	Commander US Army Tank Automotive Rsch and Development Command ATTN: DRDTA-UL Warren, MI 48090
2	Commander US Army Armament Research and Development Command ATTN: DRDAR-TSS Dover, NJ 07801
1	Commander Benet Weapons Laboratory, LCWSL US Army Armament Research and Development Command ATTN: DRDAR-LCB Watervliet, NY 12189
1	Commander US Army Armament Materiel Readiness Command ATTN: DRSAR-LEP-L, Tech Lib Rock Island, IL 61299

DISTRIBUTION LIST

No. of Copies	Organization
1	Commander US Army White Sands Missile Range ATTN: STEWS-TE-N, J. Gorman White Sands, NM 88002
5	Commander US Army Harry Diamond Labs ATTN: DELHD-TI/012 Mr. F. N. Wimenitz Mr. Jim Gaul DELHD-NP, J. Gwaltney DELHD-RBH, P.A.Caldwell 2800 Powder Mill Road Adelphi, MD 20783
1	Commander US Army Materials and Mechanics Research Center ATTN: Tech Lib Watertown, MA 02172
1	Commander US Army Natick Research and Development Command ATTN: DRXRE, Dr. D. Sieling Natick, MA 01762
1	Commander US Army Foreign Science and Technology Center ATTN: Rsch & Data Branch Federal Office Building 220 Seventh Street, NE Charlottesville, VA 22901
1	Director US Army TRADOC Systems Analysis Activity ATTN: ATAA-SL, Tech Lib White Sands Missile Range NM 88002
3	Commander US Army Nuclear Agency ATTN: ATCN-W, CPT Ader CDINS-E Technical Library 7500 Backlick Rd, Bldg. 2073 Springfield, VA 22150
1	Commander US Army Communications Command ATTN: Tech Library Fort Huachuca, AZ 85613
1	Interservice Nuclear Weapons School ATTN: Technical Library Kirtland AFB, NM 87115
2	HQDA (DAMA-MC; NCB Div) Washington, DC 20310
2	HQDA (DAEN-MC; DAEN-CWE) Washington, DC 20310
2	Office, Chief of Engineers Department of the Army Publications Department ATTN: DAEN-MCE-D DAEN-RDM 890 S. Pickett Street Alexandria, VA 22304
3	Director US Army BMD Advanced Technology Center ATTN: CRDABH-X, J. Davidson CRDABH-S, Mr. M. Capps N. J. Hurst P.O. Box 1500, West Station Huntsville, AL 35807
1	Commander US Army Research Office P. O. Box 12211 Research Triangle Park NC 27709

DISTRIBUTION LIST

No. of Copies	Organization
4	Commander US Army Engineer Waterways Experiment Station ATTN: Technical Library William Flathau John N. Strange James Ballard P. O. Box 631 Vicksburg, MS 39180
2	Director Defense Civil Preparedness Agency ATTN: Mr. George Sisson/RF-SR Technical Library Washington, DC 20301
1	Commander US Army Engineering Center ATTN: ATSEN-SY-L Fort Belvoir, VA 22060
1	Director US Army Construction Engineering Research Laboratory ATTN: CERL-SL P. O. Box 4005 Champaign, IL 61820
1	Division Engineer US Army Engineering Division ATTN: Docu Cen Ohio River, P.O. Box 1159 Cincinnati, OH 42501
1	Division Engineer US Army Engineering Division ATTN: Mr. M. Dembo Huntsville Box 1600 Huntsville, AL 35804
4	Chief of Naval Research ATTN: Code 461, Jacob L. Warner Thomas P. Quinn N. Perrone (2 cys) Department of the Navy Washington, DC 20360
2	Chief of Naval Operations ATTN: OP-03EG OP-985F Department of the Navy Washington, DC 20350
1	Chief of Naval Material ATTN: MAT-0323 Department of the Navy Arlington, VA 22217
1	Director Strategic Systems Project Ofc ATTN: NSP-43, Tech Lib Department of the Navy Washington, DC 20360
1	Commander Naval Electronic Systems Cmd ATTN: PME 117-21A Washington, DC 20360
2	Commander Naval Sea Systems Command ATTN: ORD-91313 Library Code 03511 Department of the Navy Washington, DC 20362
3	Commander Naval Facilities Engineering Command ATTN: Code 03A Code 04B Technical Library Washington, DC 20360
2	Commander Naval Ship Engineering Center ATTN: Technical Library NSEC 6105G Hyattsville, MD 20782

DISTRIBUTION LIST

No. of Copies	Organization
1	Commander David W. Taylor Naval Ship Research & Development Ctr ATTN: Lib Div., Code 522 Bethesda, MD 20084
3	Commander Naval Surface Weapons Center ATTN: Code 1224/Navy Nuclear Programs Office Code CR14, Tech Lib Francis B. Prozel Silver Spring, MD 20910
1	Commander Naval Surface Weapons Center ATTN: DX-21, Lib Br. Dahlgren, VA 22448
2	Commander Naval Ship Research and Development Center Facility Underwater Explosions Research Division ATTN: Code 14, W.W. Murray Technical Library Portsmouth, VA 23709
1	Commander Naval Weapons Evaluation Facility Kirtland AFB Albuquerque, NM 87117
2	Commander and Director Naval Civil Engineer Lab ATTN: Code L31, Mr. Shaw Mr. R. Siebold Port Hueneme, CA 93041
3	Officer-in-Charge Civil Engineering Laboratory Naval Constr Btn Center ATTN: Stan Takahashi R. J. Odello Technical Lib Port Hueneme, CA 93041
2	Commander Naval Research Laboratory ATTN: Code 2027, Tech Lib Code 8440, F. Rosenthal Washington, DC 20375
1	Superintendent Naval Postgraduate School ATTN: Code 2124, Tech Rpts Lib Monterey, CA 93940
1	HQ USAF (SAFRD) Washington, DC 20330
1	HQ USAF (INATA) Washington, DC 20330
2	AFSC (DLCAW; Tech Lib) Andrews AFB Washington, DC 20331
2	AFATL (ATRD, R. Brandt) Eglin AFB, FL 32542
1	RADC (FMTLD/Docu Lib) Griffiss AFB, NY 13340
1	AFWL (SUL) Kirtland AFB, NM 87117
3	AFWL (Robert Port; DEV Jimmie L. Bratton; DEV, M. A. Plamondon) Kirtland AFB, NM 87117
1	Commander-in-Chief Strategic Air Command ATTN: NRI-STINFO Lib Offutt AFB, NM 68113
1	AFFDL (FDTR, Dr. F.J.Janik, Jr.) Wright-Patterson AFB, OH 45433
1	AFML (LLN/Dr. T. Nicholas) Wright-Patterson AFB, OH 45433

DISTRIBUTION LIST

No. of Copies	Organization
1	FTD (TDPTN) Wright-Patterson AFB, OH 45433
1	AFIT (Lib Bldg. 640, Area B) Wright-Patterson AFB, OH 45433
1	Director US Bureau of Mines ATTN: Technical Library Denver Federal Center Denver, CO 80225
1	Director US Bureau of Mines Twin Cities Research Center ATTN: Technical Library P. O. Box 1660 Minneapolis, MN 55111
1	US Energy Research and Development Administration Division of Headquarters Svcs ATTN: Doc Control for Classified Tech Lib Library Branch G-043 Washington, DC 20545
1	US Energy Research and Development Administration Albuquerque Operations Office ATTN: Doc Control for Tech Lib P.O. Box 5400 Albuquerque, NM 87115
1	US Energy Research and Development Administration Nevada Operations Office ATTN: Doc Control for Tech Lib P. O. Box 14100 Las Vegas, NV 89114
2	Director Lawrence Livermore Laboratory ATTN: Larry W. Woodruff, L-125 Technical Info Division P. O. Box 808 Livermore, CA 94550
1	Director Los Alamos Scientific Lab ATTN: Doc Control for Rpt Lib P. O. Box 1663 Los Alamos, NM 87544
1	Director NASA Scientific and Tech Info Facility ATTN: SAK/DL P. O. Box 8757 Baltimore/Washington International Airport, MD 21240
1	National Academy of Sciences ATTN: Mr. D. G. Groves 2101 Constitution Ave, NW Washington, DC 20418
1	Agbabian Associates ATTN: M. Agbabian 250 North Nash Street El Segundo, CA 90245
2	Applied Theory, Inc. ATTN: John G. Trulio 1010 Westwood Blvd. Los Angeles, CA 90024
1	AVCO Government Products Group ATTN: Res Lib A830, Rm 7201 201 Lowell Street Wilmington, MA 01887
1	AVCO Structures & Mechanics Dept ATTN: Dr. William Broding Mr. J. Gilmore Wilmington, MA 01887
1	Bell Helicopter Textron ATTN: R. Eggers, Cobra PM P. O. Box 482 Fort Worth, TX 76101

DISTRIBUTION LIST

No. of Copies	Organization
1	Bell Telephone Labs, Inc. ATTN: Tech Rpt Ctr Mountain Avenue Murray Hill, NJ 07971
1	The Boeing Company ATTN: Aerospace Library P. O. Box 3707 Seattle, WA 98124
2	California Research and Technology, Inc. ATTN: Ken Kreyenhagen Technical Library 6269 Variel Avenue Woodland Hills, CA 91364
1	Calspan Corporation ATTN: Technical Library P. O. Box 235 Buffalo, NY 14221
1	Civil/Nuclear Systems Corp ATTN: Robert Crawford 1200 University NE Albuquerque, NM 87102
1	EG&G, Incorporated Albuquerque Division ATTN: Technical Library P. O. Box 10218 Albuquerque, NM 87114
1	General American Trans Corp. General American Res Div ATTN: G. L. Neidhardt 7449 N. Natchez Avenue Niles, IL 60648
1	General Electric Company-TEMPO ATTN: DASIAC P. O. Drawer QQ Santa Barbara, CA 93102
1	President General Research Corporation ATTN: Library McLean, VA 22101
1	Honeywell, Inc. Govt. & Aero Products Div 600 Second Street, NE Hopkins, MN 55343
1	Hughes Helicopters ATTN: A. C. Edwards Dept. 15-43 Centinela & Teale Streets Culver City, CA 90230
1	J.G. Engineering Research Associates 3831 Menlo Drive Baltimore, MD 21215
1	J.L. Merritt Consulting & Special Eng Services, Inc. ATTN: Technical Library P. O. Box 1206 Redlands, CA 92373
2	Kaman AviDyne ATTN: Dr. N. P. Hobbs Mr. S. Cricione 83 Second Avenue Northwest Industrial Park Burlington, MA 01803
2	Lockheed Missiles & Space Co. ATTN: T. Gerrs D/52-53 Bldg. 205 Tech Info Ctr, Doc/Coll. 3251 Hanover Street Palo Alto, CA 94304
1	McDonnell Douglas Corporation ATTN: Robert W. Halprin 5301 Bolsa Avenue Huntington Beach, CA 92647

DISTRIBUTION LIST

No. of Copies	Organization
1	The Mitre Corporation ATTN: Library Rt 62 & Middlesex Turnpike P. O. Box 208 Bedford, MA 01730
2	Physics International Corp. ATTN: E. T. Moore Dennis Orphas 2700 Merced Street San Leandro, CA 94577
4	Physics International Corp. ATTN: Robert Swift Charles Godfrey Larry A. Behrmann Technical Library 2700 Merced Street San Leandro, CA 94577
5	R&D Associates ATTN: Dr. H. L. Brode Dr. Albert L. Latter Bruce Hartenbaum William B. Wright Henry Cooper P. O. Box 9695 Marina del Rey, CA 90291
4	R&D Associates ATTN: Jerry Carpenter Sheldon Schuster J. G. Lewis Technical Library P. O. Box 9695 Marina del Rey, CA 90291
1	Sandia Laboratories ATTN: Doc Control for 3141 Sandia Report Coll. Albuquerque, NM 87115
2	Sandia Laboratories Livermore Laboratory ATTN: Doc Control for Tech Lib Doc Control for L. Hill P. O. Box 969 Livermore, CA 94550
1	Science Applications, Inc. ATTN: R. A. Shunk P. O. Box 3507 Albuquerque, NM 87110
3	Science Applications, Inc. ATTN: R. Seebaugh William M. Layson John Mansfield 1651 Old Meadow Road McLean, VA 22101
2	Science Applications, Inc. ATTN: David Bernstein D. E. Maxwell 2450 Washington Ave, Suite 120 San Leandro, CA 94577
2	Science Applications, Inc. ATTN: Technical Library Michael McKay P. O. Box 2351 La Jolla, CA 92038
1	Shock Hydrodynamics, Inc. A Division of Whittaker Corp. ATTN: L. Zernow 4710-16 Vineland Avenue North Hollywood, CA 91602
5	Systems, Science & Software ATTN: Robert T. Allen Donald R. Grine Ted Cherry Thomas D. Riney Technical Library P. O. Box 1620 La Jolla, CA 92037

DISTRIBUTION LIST

No. of Copies	Organization
2	Terra Tek, Inc. ATTN: Sidney Green Technical Library 420 Wakara Way Salt Lake City, UT 84108
2	Tetra Tech, Inc. ATTN: Li-San Hwang Technical Library 630 North Rosemead Blvd. Pasadena, CA 91107
7	TRW Systems Group ATTN: Paul Lieberman Benjamin Sussholtz Norm Lipner William Rowan Jack Farrell Pravin Bhutta Tech Info Ctr/S-1930 One Space Park Redondo Beach, CA 92078
2	TRW Systems Group ATTN: Mr. F. A. Pieper Greg Hulcher San Bernardino Operations P. O. Box 1310 San Bernardino, CA 92402
2	Union Carbide Corporation Holifield National Laboratory ATTN: Doc Control for Tech Lib Civil Defense Res Proj P. O. Box X Oak Ridge, TN 37830
1	Universal Analytics, Inc. ATTN: E. I. Field 7740 W. Manchester Blvd. Playa del Rey, CA 90291
1	URS Research Company ATTN: Technical Library 155 Bovet Road San Mateo, CA 94402
1	Weidlinger Assoc. Consulting Engineers ATTN: J. Isenbert 2710 San Hill Road Suite 230 Menlo Park, CA 99025
1	Westinghouse Electric Co. Marine Division ATTN: W. A. Volz Hendy Avenue Sunnyvale, CA 94008
4	Denver Research Institute University of Denver ATTN: Mr. J. Wisotski Fred P. Vanditti Ron W. Buchanon Technical Library P. O. Box 10127 Denver, CO 80210
3	IIT Research Institute ATTN: Milton R. Johnson R. E. Welch Technical Library 10 West 35th Street Chicago, IL 60616
2	Lovelace Foundation for Medical Education ATTN: Asst Dir of Research Robert K. Jones Technical Library 5200 Gibson Blvd, SE Albuquerque, NM 87108
1	Massachusetts Institute of Technology Aeroelastic and Structures Research Laboratory ATTN: Dr. E. A. Witmer Cambridge, MA 02139

DISTRIBUTION LIST

No. of Copies	Organization
2	Southwest Research Institute ATTN: Dr. W. E. Baker A. B. Wenzel 8500 Culebra Road San Antonio, TX 78206
4	Stanford Research Institute ATTN: Dr. G. R. Abrahamson Carl Peterson Burt R. Gasten SRI Library, Rm G021 333 Ravenswood Avenue Menlo Park, CA 94025
1	University of Illinois Consulting Eng. Services ATTN: Nathan M. Newmark 1114 Civil Engineering Bldg. Urbana, IL 61801
2	The University of New Mexico The Eric H. Wang Civil Engineering Rsch Facility ATTN: Larry Bickle Neal Baum University Station, Box 188 Albuquerque, NM 87131
2	Washington State University Administration Office ATTN: Arthur Miles Hohorf George Duval Pullman, WA 99163
1	University of Tennessee Space Insitute ATTN: Dr. D. R. Keefer Tullahoma, TN 37388
	Aberdeen Proving Ground
	Dir, USAMSAA ATTN: Dr. J. Sperrazza Mr. R. Norman, GWD Dr. Rivello R. Bailey DRXSY-MP, H. Cohen
	Cdr, USATECOM ATTN: DRSTE-SG-H